

Neutrino mixing in matter

S. H. Chiu,^{1,*} T. K. Kuo,^{2,†} and Lu-Xin Liu^{2,3,‡}

¹*Physics Group, CGE, Chang Gung University, Kwei-Shan 333, Taiwan*

²*Department of Physics, Purdue University, West Lafayette, IN 47907, USA*

³*National Institute for Theoretical Physics, Department of Physics and Centre for Theoretical Physics, University of the Witwatersrand, Wits, 2050, South Africa*

Three-neutrino mixing in matter is studied through a set of evolution equations which are based on a rephasing invariant parametrization. Making use of the known properties of measured neutrino parameters, analytic, approximate solutions are obtained. Their accuracy is confirmed by comparison with numerical integration of these equations. The results, when expressed in the elements squared of the mixing matrix, exhibit striking patterns as the matter density varies.

PACS numbers: 14.60.Pq, 14.60.Lm, 13.15.+g

It is well-established that neutrino mixing is modified by the presence of matter [1]. Their effect has been used in the analyses of solar neutrinos, and is expected to impact those of the supernova neutrinos, when and if they become available. Closer to home, there is a plethora of long baseline experiments either in operation or in the planning stage. For these studies, it is essential to include the matter effects in order to understand neutrino mixing at the fundamental level.

In the literature, effort has been devoted to solving problems along this line [2]. However, the process involves the complication of the cubic eigenvalue problems, and the results are usually far from transparent for a clear extraction of the physical implications.

In this work we derive a set of evolution equations for the neutrino parameters, using a rephasing invariant parametrization which was developed for three-flavor quark mixing. The same formalism can be used in the neutrino sector, as long as it is used for lepton number conserving processes, such as in neutrino oscillation, which will be studied here. It will be shown that the coupled equations have simple, analytic, solutions which, when compared to the complete numerical solutions, are quite accurate.

For the neutrino mixing (PMNS) matrix (V), we adopt the parametrization introduced earlier [3]. Briefly, without loss of generality, one can demand $\det V = +1$. There are then a set of rephasing invariants

$$\Gamma_{ijk} = V_{1i}V_{2j}V_{3k} = R_{ijk} - iJ, \quad (1)$$

where their common imaginary part can be identified with the Jarlskog invariant J [4]. Their real parts were defined as

$$(R_{123}, R_{231}, R_{312}; R_{132}, R_{213}, R_{321}) = (x_1, x_2, x_3; y_1, y_2, y_3). \quad (2)$$

These variables are bounded by ± 1 : $-1 \leq (x_i, y_j) \leq +1$, with $y_j \leq x_i$ for any (i, j) . They satisfy two constraints

$$\det V = (x_1 + x_2 + x_3) - (y_1 + y_2 + y_3) = 1, \quad (3)$$

$$(x_1x_2 + x_2x_3 + x_3x_1) - (y_1y_2 + y_2y_3 + y_3y_1) = 0. \quad (4)$$

In addition, it is found that

$$J^2 = x_1x_2x_3 - y_1y_2y_3. \quad (5)$$

The (x, y) parameters are related to $|V_{ij}|^2$ by

$$W = [|V_{ij}|^2] = \begin{pmatrix} x_1 - y_1 & x_2 - y_2 & x_3 - y_3 \\ x_3 - y_2 & x_1 - y_3 & x_2 - y_1 \\ x_2 - y_3 & x_3 - y_1 & x_1 - y_2 \end{pmatrix}. \quad (6)$$

One can readily obtain the parameters (x, y) from W by computing its cofactors, which form the matrix w with $w^T W = (\det W)I$, and is given by

$$w = \begin{pmatrix} x_1 + y_1 & x_2 + y_2 & x_3 + y_3 \\ x_3 + y_2 & x_1 + y_3 & x_2 + y_1 \\ x_2 + y_3 & x_3 + y_1 & x_1 + y_2 \end{pmatrix}. \quad (7)$$

Physical measurables can always be expressed in terms of (x, y) . For instance, the $\nu_\mu \rightarrow \nu_e$ transition probability is given by

$$\begin{aligned} P(\nu_\mu \rightarrow \nu_e) = & -4[F_{21}^{\mu e} \sin^2(\frac{D_2 - D_1}{4E/L}) \\ & + F_{31}^{\mu e} \sin^2(\frac{D_3 - D_1}{4E/L}) + F_{32}^{\mu e} \sin^2(\frac{D_3 - D_2}{4E/L})] \\ & + 8J \sin(\frac{D_2 - D_1}{4E/L}) \sin(\frac{D_3 - D_1}{4E/L}) \sin(\frac{D_3 - D_2}{4E/L}), \end{aligned} \quad (8)$$

where D_i = neutrino mass squared, L is the length of baseline, E is the neutrino energy, and

$$\begin{aligned} x_2x_3 + x_1y_2 - y_1y_2 - y_2y_3 & \equiv F_{21}^{\mu e}, \\ -x_1x_3 - x_2x_3 + x_3y_1 + y_2y_3 & \equiv F_{31}^{\mu e}, \\ x_1x_3 + x_2y_3 - y_1y_3 - y_2y_3 & \equiv F_{32}^{\mu e}. \end{aligned} \quad (9)$$

*Electronic address: schiu@mail.cgu.edu.tw

†Electronic address: tkkuo@purdue.edu

‡Electronic address: Luxin.Liu@wits.ac.za

Experimentally, the PMNS matrix in vacuum is well-approximated by

$$W_0 = \begin{pmatrix} \frac{2(1-\epsilon^2)}{3} - 2\eta & \frac{1-\epsilon^2}{3} + 2\eta & \epsilon^2 \\ \frac{1+2\epsilon^2-\xi}{6} + \beta + \eta & \frac{2+\epsilon^2-2\xi}{6} - \beta - \eta & \frac{1-\epsilon^2+\xi}{2} \\ \frac{1+2\epsilon^2+\xi}{6} - \beta + \eta & \frac{2+\epsilon^2+2\xi}{6} + \beta - \eta & \frac{1-\epsilon^2-\xi}{2} \end{pmatrix} \quad (10)$$

with $(\epsilon, \eta, \beta, \xi) \ll 1$. W_0 reduces to the tri-bimaximal [5] matrix when $\epsilon = \eta = \beta = \xi = 0$. If we allow the parameters $(\epsilon, \eta, \beta, \xi)$ to take on arbitrary values, the matrix above can be used as a general parametrization of the mixing matrix. Also, it is related to the familiar “standard parametrization” [6] by $S_{13}^2 = \epsilon^2$, $S_{12}^2 = \frac{1}{3} + \frac{2\eta}{1-\epsilon^2}$, $S_{23}^2 = \frac{1}{2} + \frac{1}{2} \frac{\xi}{1-\epsilon^2}$, and β is a complicated function but $\beta \simeq \frac{\sqrt{2}}{3} C_\phi S_{13}$ for $(\epsilon, \eta, \xi) \ll 1$. From W_0 , we find readily $x_{10} \simeq 1/3$, $x_{20} \simeq 1/6$, $x_{30} \simeq 0$, and $x_{i0} + y_{i0} \simeq 0$ ($i = 1, 2, 3$).

In the flavor basis, the effective Hamiltonian for neutrinos propagating in matter is given by $H_{\text{eff}} = \frac{H}{2E}$,

$$H = \left[V_0 \begin{pmatrix} m_1^2 & & \\ & m_2^2 & \\ & & m_3^2 \end{pmatrix} V_0^\dagger + \begin{pmatrix} A & & \\ & 0 & \\ & & 0 \end{pmatrix} \right], \quad (11)$$

where m_1 , m_2 , and m_3 are the neutrino masses in vacuum, V_0 is the mixing matrix in vacuum, and the induced mass $A = \sqrt{2} G_F n_e E$.

The matrix H can be diagonalized,

$$H = V D V^\dagger = V \begin{pmatrix} D_1 & & \\ & D_2 & \\ & & D_3 \end{pmatrix} V^\dagger, \quad (12)$$

where $D_i = M_i^2$ is the squared mass in matter. To study how the elements of V evolve in matter, one may start with dH/dA ,

$$\frac{dH}{dA} = \frac{d}{dA} [V D V^\dagger] = \begin{pmatrix} 1 & & \\ & 0 & \\ & & 0 \end{pmatrix}. \quad (13)$$

Eq. (13) is then sandwiched by V^\dagger and V ,

$$V^\dagger \frac{dV}{dA} D + \frac{dD}{dA} + D \frac{dV^\dagger}{dA} V = \begin{pmatrix} |V_{11}|^2 & V_{12} V_{11}^* & V_{13} V_{11}^* \\ V_{11} V_{12}^* & |V_{12}|^2 & V_{13} V_{12}^* \\ V_{11} V_{13}^* & V_{12} V_{13}^* & |V_{13}|^2 \end{pmatrix}. \quad (14)$$

Taking the diagonal and off-diagonal terms of Eq. (14), and following the procedures in Ref.[7], we find

$$\frac{dD_i}{dA} = |V_{1i}|^2 = x_i - y_i, \quad (i = 1, 2, 3) \quad (15)$$

$$\frac{dV_{ij}}{dA} = \sum_{k \neq j} \frac{V_{ik} V_{1j}}{D_j - D_k} V_{1k}^*. \quad (16)$$

Eq. (16) follows from $[(dV^\dagger/dA)V]_{ik} = V_{1i}^* V_{ik}/(D_i - D_k)$, $i \neq k$, which can be inverted to solve for dV/dA since the

unknown element $[(dV^\dagger/dA)V]_{ii}$ is rephasing dependent, and can be set to vanish.

While Eq. (16) is rephasing dependent, it may be used to compute rephasing invariant quantities, *e.g.*,

$$\frac{d\Gamma_{123}}{dA} = \frac{d}{dA} (V_{11} V_{22} V_{33}) = \frac{dx_1}{dA} - i \frac{dJ}{dA}. \quad (17)$$

After some algebra, separating the real and imaginary parts, in addition to using different Γ'_{ijk} s, we obtain the evolution equations for all (x_i, y_i) and $d \ln J/dA$, which are collected in Table I. The evolution equations obtained here are entirely analogous to the familiar RGE of mass matrices. In both cases, the effective Hamiltonian contains a parameter, the energy for RGE, and A for neutrino propagation. The respective evolution equations can be used to solve for eigenvalues and mixings as functions either of the energy scale, or of A .

The symmetric form of these equations allows us to find readily the result:

$$\frac{d}{dA} \ln [J(D_1 - D_2)(D_2 - D_3)(D_3 - D_1)] = 0, \quad (18)$$

i.e., the product $[J(D_1 - D_2)(D_2 - D_3)(D_3 - D_1)]$ is a constant as A changes, a well-known result derived with different methods [9].

In addition, by writing down the evolution equations for $(d/dA) \ln(x_i - y_i)$, from Table I, we find another “matter invariant”:

$$\frac{d}{dA} \left[\frac{J^2}{(x_1 - y_1)(x_2 - y_2)(x_3 - y_3)} \right] = 0. \quad (19)$$

Or, $[J^2/(|V_{11}|^2 |V_{12}|^2 |V_{13}|^2)] = \text{constant}$. When we use the “standard parametrization”, it is seen that $J^2/(|V_{11}|^2 |V_{12}|^2 |V_{13}|^2) = S_\phi^2 S_{23}^2 C_{23}^2$, *i.e.*, $S_\phi \sin 2\theta_{23}$ is independent of A , a result obtained earlier [11].

The evolution equations for (x, y) also have a structure akin to that of the fixed point of single variable equations. It can be verified that, if $x_i + y_i = 0$ ($i = 1, 2, 3$), then

$$\frac{d}{dA} (x_j + y_j) = 0, \quad j = (1, 2, 3). \quad (20)$$

This result is understandable since the conditions $x_i + y_i = 0$ are equivalent to $W_{2i} = W_{3i}$, which, in turn, imply that the effective Hamiltonian H has a $\mu - \tau$ exchange symmetry [8]. This symmetry is clearly independent of A in Eq. (11), resulting in Eq. (20). Note also that there are actually only two independent constraints in $x_i + y_i = 0$. Given any two of them, say for $i = 1, 2$, we can use Eq.(4) to derive $x_3 + y_3 = 0$. Thus, the set of evolution equations has a “fixed surface”, points on the surface defined by $x_i + y_i = 0$ stay on it as A varies.

While analytical solutions to the equations in Table 1 are not available, as we will see, given the known physical parameters, one can exploit certain characteristic properties thereof to arrive at simple, but fairly accurate, solutions to these equations.

	$1/(D_1 - D_2)$	$1/(D_2 - D_3)$	$1/(D_3 - D_1)$
dx_1/dA	$x_1x_2 - 2x_1y_2 + y_1y_2$	$-x_1x_2 + x_1x_3 + y_1y_2 - y_1y_3$	$-x_1x_3 + 2x_1y_3 - y_1y_3$
dx_2/dA	$-x_1x_2 + 2x_2y_1 - y_1y_2$	$x_2x_3 - 2x_2y_3 + y_2y_3$	$x_1x_2 - x_2x_3 - y_1y_2 + y_2y_3$
dx_3/dA	$-x_1x_3 + x_2x_3 + y_1y_3 - y_2y_3$	$-x_2x_3 + 2x_3y_2 - y_2y_3$	$x_1x_3 - 2x_3y_1 + y_1y_3$
dy_1/dA	$-x_1x_2 + 2x_2y_1 - y_1y_2$	$-x_1x_2 + x_1x_3 + y_1y_2 - y_1y_3$	$x_1x_3 - 2x_3y_1 + y_1y_3$
dy_2/dA	$x_1x_2 - 2x_1y_2 + y_1y_2$	$-x_2x_3 + 2x_3y_2 - y_2y_3$	$x_1x_2 - x_2x_3 - y_1y_2 + y_2y_3$
dy_3/dA	$-x_1x_3 + x_2x_3 + y_1y_3 - y_2y_3$	$x_2x_3 - 2x_2y_3 + y_2y_3$	$-x_1x_3 + 2x_1y_3 - y_1y_3$
$d(\ln J)/dA$	$-x_1 + x_2 + y_1 - y_2$	$-x_2 + x_3 + y_2 - y_3$	$x_1 - x_3 - y_1 + y_3$

TABLE I: dx_i/dA , dy_i/dA , and $d(\ln J)/dA$ are expressed as sums of terms in $1/(D_1 - D_2)$, $1/(D_2 - D_3)$, and $1/(D_3 - D_1)$.

Experimentally, it is known that $\delta_0 = m_2^2 - m_1^2 \cong 7 \times 10^{-5} eV^2$, $\Delta_0 = m_3^2 - m_2^2 \cong 3 \times 10^{-3} eV^2$, so that $\delta_0/\Delta_0 \ll 1$ (we assume the “normal” ordering of neutrino masses. The “inverted” case can be similarly treated). Note that these values are relevant to long baseline experiments since $A = \sqrt{2} G_F n_e E \sim (7.6 \times 10^{-5} eV^2)(E/GeV)(\rho/gcm^{-3})$.

Since $\delta_0 \ll \Delta_0$, we expect that the three-flavor problem can be approximated by a pair of well separated two-flavor problems [10]. Indeed, the structure of the differential equations in Table I shows that the variables (x_i, y_i) evolve slowly as a function of A except for two regions, where $D_1 \approx D_2$ and $D_2 \approx D_3$, corresponding to the two resonance regions. More precisely, let us denote by $(A_0, A_l, A_i, A_h, A_d)$ the values of A in vacuum ($A_0 = 0$), at the lower resonance ($A_l, [d(D_1 - D_2)/dA]_{A_l} = 0$), intermediate range (A_i), higher resonance ($A_h, [d(D_2 - D_3)/dA]_{A_h} = 0$), and for dense medium (A_d). Rapid evolution for (x_i, y_i) only occurs for $A \approx A_l$ and $A \approx A_h$.

For $0 \leq A < A_i$, we need only to keep the terms $\propto 1/(D_1 - D_2)$ in Table I. It is seen that

$$\frac{d(x_1 - y_2)}{dA} = \frac{d(x_2 - y_1)}{dA} = \frac{d(x_3 - y_3)}{dA} = 0. \quad (21)$$

Given W_0 (Eq. (10)), with $x_{i0} + y_{i0} \cong 0$, Eq. (20) yields $x_i + y_i \cong 0$. Thus, we expect that for $0 \leq A < A_i$, while the individual variables (x_1, x_2, y_1, y_2) are rapidly changing, $x_3 \simeq y_3 \simeq \mathcal{O}(\epsilon)$ stay small, as do the combinations $x_1 + y_1 \cong x_2 + y_2 \cong 0$, and $x_1 + x_2 \simeq \text{constant}$, $y_1 + y_2 \simeq \text{constant}$. The differential equations can then be approximated, with $\delta \equiv D_2 - D_1$, by

$$\frac{dx_1}{dA} \cong \frac{-4x_1x_2}{\delta} \cong -\frac{dx_2}{dA}, \quad \frac{d\delta}{dA} \cong 2(x_2 - x_1). \quad (22)$$

It follows that

$$\begin{aligned} \frac{d}{dA}[x_1x_2\delta^2] &= 0, \\ \frac{d}{dA}[(x_1 - x_2)\delta] &= -2(x_1 + x_2)^2 \equiv -b_l, \end{aligned} \quad (23)$$

where $b_l \cong 2(x_{10} + x_{20})^2$. So, in the lower resonance

region, the explicit, approximate, solutions are

$$\begin{aligned} \delta &= [2b_l A^2 - 4c_l A + \delta_0^2]^{1/2}, \\ x_1 &= \frac{1}{2}[(x_{10} + x_{20}) - (b_l A - c_l)/\delta], \\ x_2 &= \frac{1}{2}[(x_{10} + x_{20}) + (b_l A - c_l)/\delta], \end{aligned} \quad (24)$$

with $c_l = \delta_0(x_{10} - x_{20})$. Also, $x_1 + y_1 \cong x_2 + y_2 \cong 0$, $x_3 \cong y_3 \cong 0$. From W_0 , we have $b_l = 2(x_{10} + x_{20})^2 \cong 1/2$. We see thus, as A sweeps through the lower resonance region, δ goes through a minimum, x_1 decreases and x_2 rises while keeping $x_1 + x_2 \simeq 1/2$. After the resonance, for large A ($A \gg \delta_0$), $\delta \simeq A$, $x_1 \rightarrow 0$, and $x_2 \rightarrow 1/2$.

A similar analysis can be done for the region $A_i < A < A_d$. Here, the starting values ($A_l \ll A < A_h$) are $x_1 \simeq y_1 \simeq 0$, $x_3 \simeq y_3 \simeq 0$, $x_2 \rightarrow 1/2$, $y_2 \rightarrow -1/2$. The differential equations are dominated by terms proportional to $1/(D_2 - D_3)$, and they satisfy

$$\frac{d(x_1 - y_1)}{dA} = \frac{d(x_2 - y_3)}{dA} = \frac{d(x_3 - y_2)}{dA} = 0. \quad (25)$$

With $\Delta \equiv D_3 - D_2$, the approximate equations near $A \approx A_h$ are then

$$\frac{dx_2}{dA} \cong \frac{-4x_2x_3}{\Delta} \cong -\frac{dx_3}{dA}, \quad \frac{d\Delta}{dA} \cong 2(x_3 - x_2), \quad (26)$$

together with $x_2 + y_2 \simeq x_3 + y_3 \simeq 0$, while x_1 and y_1 are slowly varying so that $x_1 \simeq y_1 \simeq 0$ throughout.

The solutions are

$$\begin{aligned} \Delta &= [2b_h A^2 - 4c_h A + \Delta_0^2]^{1/2}, \\ x_2 &= \frac{1}{2}[(x_{20} + x_{30}) - (b_h A - c_h)/\Delta], \\ x_3 &= \frac{1}{2}[(x_{20} + x_{30}) + (b_h A - c_h)/\Delta], \end{aligned} \quad (27)$$

with $b_h = 2(x_{20} + x_{30})^2$ and $c_h = \Delta_0(x_{20} - x_{30})$.

Thus, as A goes from A_i through A_h to A_d , the changes for (x_i, y_j) are: $x_2 \simeq 1/2 \rightarrow 0$; $y_2 \simeq -1/2 \rightarrow 0$; $x_3 \simeq 0 \rightarrow 1/2$; and $y_3 \simeq 0 \rightarrow -1/2$.

Our results can be summarized by the matrices W at

FIG. 1: Numerical (solid) and approximate (dot-dashed) solutions for (a) all $D_3(A)$, $D_2(A)$, and $D_1(A)$, and (b) the enlarged plot of $D_2(A)$ and $D_1(A)$ in $0 \leq A/\delta_0 \leq 10$.

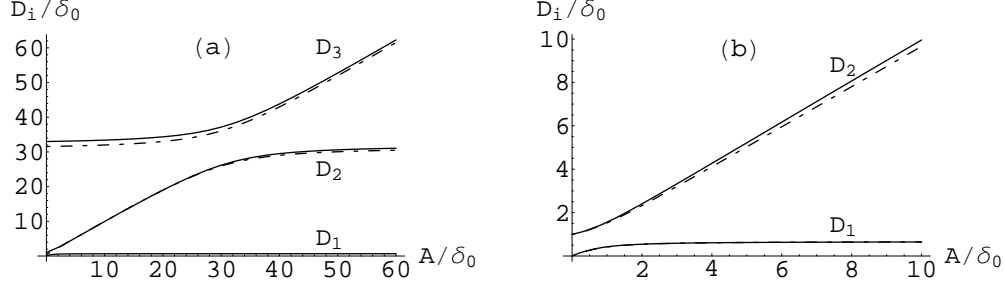
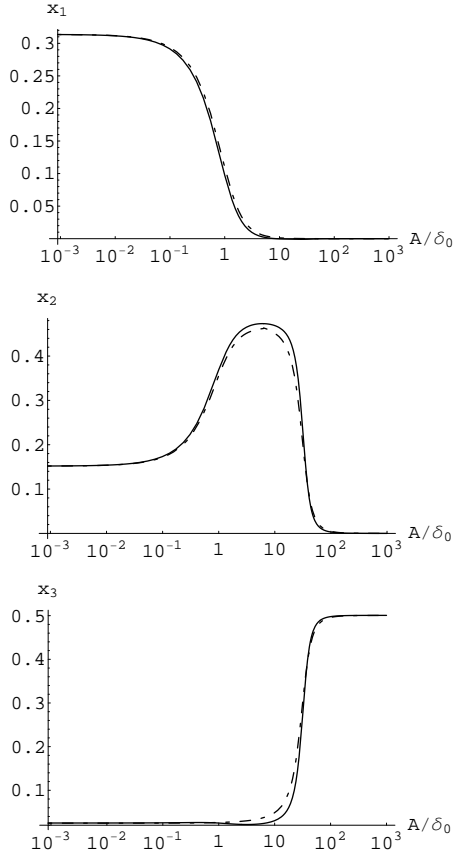


FIG. 2: The numerical (solid) and approximate (dot-dashed) solutions for $x_1(A)$, $x_2(A)$, and $x_3(A)$. Note that $y_i(A) \simeq -x_i(A)$.



$A = (A_0, A_l, A_i, A_h, A_d)$:

$$W_0 \cong \begin{pmatrix} 2/3 & 1/3 & 0 \\ 1/6 & 1/3 & 1/2 \\ 1/6 & 1/3 & 1/2 \end{pmatrix}, \quad W_l \cong \begin{pmatrix} 1/2 & 1/2 & 0 \\ 1/4 & 1/4 & 1/2 \\ 1/4 & 1/4 & 1/2 \end{pmatrix},$$

$$W_i \cong \begin{pmatrix} 0 & 1 & 0 \\ 1/2 & 0 & 1/2 \\ 1/2 & 0 & 1/2 \end{pmatrix}, \quad W_h \cong \begin{pmatrix} 0 & 1/2 & 1/2 \\ 1/2 & 1/4 & 1/4 \\ 1/2 & 1/4 & 1/4 \end{pmatrix},$$

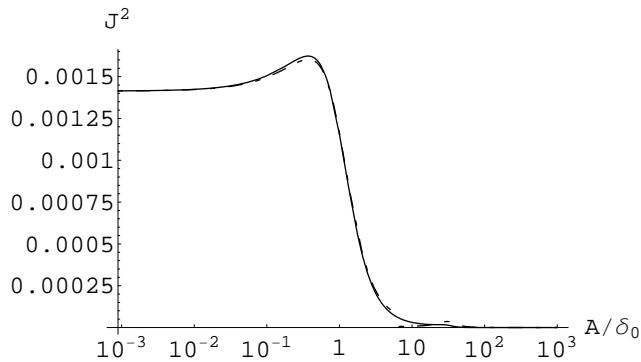
$$W_d \cong \begin{pmatrix} 0 & 0 & 1 \\ 1/2 & 1/2 & 0 \\ 1/2 & 1/2 & 0 \end{pmatrix}. \quad (28)$$

Together, these matrices exhibit the remarkable simplicity of the PMNS matrix as A varies from 0 to ∞ . Note that all of the matrices have at least one zero, $W_{lI} = 0$, implying $x_I = y_I = 0$. Also, they have equal elements in their second and third rows, $W_{2i} = W_{3i}$, so that $w_{1i} = 0$ or $x_i + y_i = 0$. As a consequence, using the unitarity conditions, the W matrix is completely fixed by its elements in the first row, W_{1i} . These elements, in turn, control dD_i/dA , Eq. (15). Thus, the progression of W as a function of A can be read off from the plot of $D_i(A)$, which is given in Fig. 1.

It is straightforward to numerically integrate the evolution equations for (x, y) . To do this we choose the initial values (in W_0) $\epsilon = 0.17$, $\beta = 0.02$, corresponding to the experimental bounds $|V_{e3}|^2 \leq 0.03$ [6] and an assumed CP violation phase $\cos \phi = 1/4$. Also, $\xi = \eta = 0$. In Fig. 2 the results are compared to the approximate solutions obtained earlier (Eqs. (24) and (27)). The agreements are quite good. The evolution of J^2 is shown in Fig. 3. Compared to its vacuum value, it is seen that, except for some enhancement near $A = A_l$, J^2 tends to decrease with increasing A , as one would expect from Eq. (18).

In conclusion, in this work we derived the evolution equations for the neutrino parameters as a function of matter density. We found analytic, approximate, but simple solutions of these equations for values centered around the known neutrino parameters. This is possible because of two fortuitous circumstances: 1) the neutrino mass differences are widely separated, enabling one to use the two-flavor resonance approximation; 2) the mixing in

FIG. 3: The evolution of J^2 from the numerical (solid) and the approximate (dot-dashed) solutions.



vacuum satisfies $x_{i0} + y_{i0} \cong 0$, which happens to lie on the “fixed surface” of the evolution equations, so that $x_i + y_i \cong 0$ for all A values. These solutions are summarized in Eq. (28), which exhibits the extraordinary simplicity of W as a function of A . These results are found to be quite accurate when we compare them to those obtained by numerical integration of the equations. It is hoped that they will be useful in assessing the matter effects in connection with the long baseline experiments, as well as efforts to determine CP-violation in the leptonic sector.

S.H.C. is supported by the National Science Council of Taiwan, grant No. NSC 98-2112-M-182-001-MY2.

-
- [1] S. P. Mikheyev and A. Yu. Smirnov, *Yad. Fiz.* **42**, 1441 (1985); *Sov. J. Nucl. Phys.* **42**, 913 (1985); S. P. Mikheyev and A. Yu. Smirnov, *Nuovo Cimento C* **9**, 17 (1986); L. Wolfenstein, *Phys. Rev. D* **17**, 2369 (1978).
 - [2] V. Barger, K. Whisnant, S. Pakvasa, and R. J. N. Phillips, *Phys. Rev. D* **22**, 2718 (1980); H. W. Zaglauer and K. H. Schwarzer, *Z. Phys. C* **40**, 273 (1988); Zhi-zhong Xing, *Phys. Lett. B* **487**, 327 (2000); M. Freund, *Phys. Rev. D* **64**, 053003 (2001); T. Ohlsson and H. Snellman, *J. Math. Phys.* **41**, 2768 (2000), *Erratum-ibid.* **42**, 2345 (2001).
 - [3] T. K. Kuo and T.-H. Lee, *Phys. Rev. D* **71**, 093001 (2005).
 - [4] C. Jarlskog, *Phys. Rev. Lett.* **55**, 1039 (1985).
 - [5] P. F. Harrison, D. H. Perkins, and W. G. Scott, *Phys. Lett. B* **530**, 167 (2002).
 - [6] Particle Data Group, *Phys. Lett. B* **592**, 130 (2004). Note that the phase angle “ δ ” is changed to “ ϕ ” in this paper.
 - [7] S. H. Chiu, T. K. Kuo, T.-H. Lee, and C. Xiong, *Phys. Rev. D* **79**, 013012 (2009).
 - [8] C. S. Lam, *Phys. Lett. B* **507**, 214 (2001); P. F. Harrison and W. G. Scott, *Phys. Lett. B* **547**, 219 (2002).
 - [9] P. F. Harrison and W. G. Scott, *Phys. Lett. B* **476**, 349 (2000); V. A. Naumov, *Phys. Lett. B* **323**, 351 (1994); K. Kimura, A. Takamura, and H. Yokomakura, *Phys. Lett. B* **537**, 86 (2002).
 - [10] T. K. Kuo and J. Pantaleone, *Rev. Mod. Phys.* **61**, 937 (1989).
 - [11] S. Toshev, *Mod. Phys. Lett. A* **6**, 455 (1991); P. I. Krastev and S. T. Petcov, *Phys. Lett. B* **205**, 84 (1988).